

Formulation of a direct displacement-based design procedure for steel eccentrically braced frame structures



T.J. Sullivan

*Dept. Civil Engineering and Architecture, University of Pavia, Pavia, Italy
EUCENTRE, Pavia, Italy*

SUMMARY:

The Direct displacement-based design (DBD) procedure of Priestley and co-workers has been well developed and tested for a large number of structural typologies and materials. However, development of the approach for steel structures, and in particular eccentrically braced frame (EBF) structures, has been relatively limited. In this paper, a Direct DBD procedure for steel EBF structures is formulated. New expressions are proposed for the yield drift and the design displacement profiles of EBFs with centrally located links. Reference is made to the literature for identification of suitable deformation limits and equivalent viscous damping expressions. The trial procedure is then applied to a 10-storey EBF structure and non-linear time-history analyses are undertaken to gauge the performance of the methodology. Results of the analyses indicate that the trial methodology performs reasonably well but future research is required to further develop and test the approach.

Keywords: Eccentrically braced frame, EBF, displacement based design,

1. INTRODUCTION

Seismic design procedures have received considerable attention over the past two decades as it has been recognised that there are a number of conceptual limitations with force-based design methods included in current codes (Priestley 1993, Priestley et al. 2007) and therefore a number of displacement-based design (DBD) procedures have been proposed (see Sullivan et al. 2003). Of the numerous DBD procedures in the literature, the Direct DBD procedure of Priestley and others has been developed most, with a text (Priestley et al. 2007) and a model code (Sullivan et al. 2012) on the subject. The Direct DBD procedure has been well developed for a number of structural typologies but developments for the seismic design of steel structures are relatively limited, focussing principally on steel concentrically braced frames (Della Corte and Mazzolani 2008, Wijesundara 2009, Goggins and Sullivan 2010, Salawdeh 2012) and moment-resisting frames (Sullivan et al. 2011). In this paper a possible means of applying Direct DBD to steel eccentrically braced frames will be presented.

The design and behaviour of eccentrically braced frame (EBF) structures have been well studied in the past, with research by Roeder and Popov (1977), Whittaker et al. (1987), Engelhardt and Popov (1989) and Chao and Goel (2005) to name a few. This work will focus on the design and behaviour of EBFs with centrally located links. The design philosophy to be adopted for EBF structures is to permit yielding of the short links and to design the remaining elements in the structure to remain elastic. As shown in Engelhardt and Popov (1989), the deformation capacity of the links will depend on their length, with short links, that yield in shear, being able to sustain much larger rotations than longer links that yield in flexure. As will become evident later in this paper, Direct DBD could provide a rational means of setting the strength of an EBF structure so that the link deformation demands can be effectively controlled.

2. FUNDAMENTALS OF DIRECT DBD

The main phases of the Direct DBD approach of Priestley et al. (2007) are illustrated in Figure 2.1. The approach is based on the substitute structure concept (Shibata and Sozen, 1976), whereby the MDOF structure is represented by an equivalent SDOF system, as shown in Figure 2.1a. The equivalent SDOF system is characterised by an effective stiffness, K_e , equal to the secant stiffness at peak displacement response (as shown in Figure 2.1b) an effective mass, m_e , an effective height, H_e , and an equivalent viscous damping value, ξ . The Direct DBD procedure begins by selecting a design displacement, Δ_d , intended to satisfy target performance criteria that could be storey drift limits, section curvature limits, chord rotation limits or even residual deformation limits (see Sullivan et al. 2012 for a summary of different limits possible for various structural typologies).

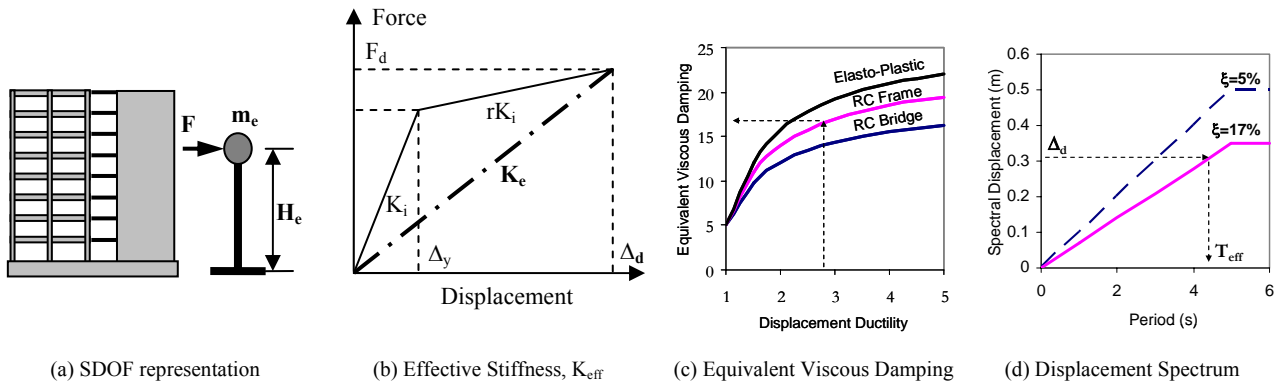


Figure 2.1. Fundamentals of Direct displacement-based seismic design (adapted from Priestley et al. 2007)

An estimate of the system ductility demand associated with the design displacement is then made, and from this, a ductility-dependent equivalent viscous damping value can be obtained as per Figure 2.1c. The equivalent viscous damping value is intended to account for the differences between the actual non-linear response of the system and the linear response associated with the use of the secant stiffness at the design displacement. Note that the equivalent viscous damping expressions used in modern Direct DBD procedures are formed after numerous non-linear dynamic analyses undertaken to calibrate the ductility-dependent equivalent viscous damping expressions for specific hysteretic models (see Pennucci et al. 2011 for discussion).

The equivalent viscous damping is used to scale the design displacement spectrum, as shown in Figure 2.1d. There are various expressions in the literature in order to scale response spectra to different levels of damping. As has been shown by Pennucci et al. (2011), care should be taken to ensure that the adopted scaling expression is representative of the ground motions used to develop the equivalent viscous damping curves. In this work the following expression is used to create a highly damped displacement spectrum, $S_{d,\xi}$, from the 5% elastic spectral displacement demands, $S_{d,5\%}$:

$$S_{d,\xi} = S_{d,5\%} \left(\frac{7}{2 + \xi} \right)^{0.5} \quad (2.1)$$

where ξ is the design value of the equivalent viscous damping.

With the highly damped displacement spectrum established, the design displacement is then used to read off a required effective period for the substitute structure, as shown in Figure 2.1d. The effective period, T_e , together with the effective mass, m_e , give the required effective stiffness, K_e , and design base shear, V_b , as per Eqn.2.2.

$$K_e = 4\pi^2 \frac{m_e}{T_e^2} \rightarrow V_b = K_e \Delta_d + C \frac{m_e g \cdot \Delta_d}{H_e} \quad (2.2)$$

where the last term in the base shear calculation is intended to account for P-delta effects, with g being the acceleration due to gravity, C is a coefficient that is typically taken equal to 1.0 for steel structures, and all the other symbols have been defined above.

The design strengths of plastic hinges can then be found by analysing the structure under a set of equivalent lateral forces given by Eqn.2.3.

$$F_i = \frac{m_i \Delta_i}{\sum m_i \Delta_i} V_b \quad (2.3)$$

Note that for frame structures, Eqn. 2.3 is usually modified such that 10% of the design base shear is lumped at roof level with the remainder distributed as per Eqn.2.3. Capacity design then provides the design forces for other elements and also for capacity-protected actions in plastic hinge regions.

This brief description of the methodology demonstrates that it is relatively straightforward. Any difficulty that exists tends to be related with the identification of the substitute structure properties. To this extent, note that the equivalent SDOF properties of design displacement, effective mass and effective height are related to the design displacement profile, as shown in Eqns. 2.4 to 2.6.

$$\Delta_d = \frac{\sum m_i \Delta_i^2}{\sum m_i \Delta_i} \quad (2.4)$$

$$m_e = \frac{\sum m_i \Delta_i}{\Delta_d} \quad (2.5)$$

$$H_e = \frac{\sum m_i \Delta_i h_i}{\sum m_i \Delta_i} \quad (2.6)$$

where Δ_i is the design displacement, m_i is the seismic mass, and h_i is the height, of level i .

3. PROPOSED DIRECT DBD PROCEDURE FOR EBF STRUCTURES

Extension of the Direct DBD procedure to EBF structures requires an expression for the design displacement profile and the equivalent viscous damping at the design limit state. In order to establish the equivalent viscous damping one requires a means of estimating the system ductility demand and should also know the hysteretic characteristics of the structure. Whereas, in order to set the design displacement profile, one needs to be able to relate local deformation limits to storey displacements that can then scale a deformed shape equation. A trial means of establishing both the design displaced shape and the equivalent viscous damping are explained in the next sub-sections.

3.1. Design Displacement Profile of EBF Structures

When EBF structures are subject to lateral loading the storey shear will cause braces to deform axially and a concave type deformation profile could be expected, with greatest shear demands occurring over the lower storeys of the building. However, in addition to shear deformations, the overturning demands will cause large axial forces in columns, and the axial deformations of columns will tend to

cause the frame to deform with a cantilever type profile. As such, identifying a simple reliable expression for the deformed shape of EBF structures is not straightforward.

Results of shake table testing undertaken on a steel EBF structure that are reported by Whittaker et al. (1987), indicated a relatively linear displacement profile at low intensities, tending towards a concave profile at large intensities. In line with this, for preliminary design, the following design displacement profile is to be trialled:

$$\Delta_i = \omega_\theta \theta_y h_i + \omega_\theta (\theta_c - \theta_y) h_i \cdot \frac{(2H_n - h_i)}{(2H_n - h_1)} \quad (3.1)$$

Where h_i is the height of level i above the base, H_n is the total building height, h_1 is the height of the 1st storey, θ_y is the minimum storey yield drift over the height of the structure and θ_c is the critical storey drift limit. The critical storey drift limit, θ_c , should be taken as the minimum value of the non-structural drift limit, $\theta_{c,ns}$, or structural storey drift limit, $\theta_{c,str}$, over the height of the EBF structure. It is also recommended that ω_θ , the higher mode drift reduction factor, be set equal to 1.0 for EBF structures of up to 6-storeys in height and should then reduce linearly with the number of storeys to a value of 0.6 for buildings of 15 storeys in height. The large reduction proposed for taller buildings recognises the potentially large contribution of higher modes to deformations of taller EBF structures.

As alluded to above, the design of steel EBF systems should consider the performance requirements of both structural and non-structural elements. Non-structural storey drift requirements should be taken as for other building systems and as such, a storey drift limit of $\theta_{c,ns} = 2.0\%$ to 2.5% could be deemed appropriate for the ultimate limit state. For the serviceability limit state, a non-structural drift limit of between $\theta_{c,ns} = 0.5\%$ to $\theta_{c,ns} = 1.0\%$ could be adopted, depending on the detailing adopted for non-structural elements (see Sullivan et al. 2012).

For structural deformation limits, Engelhardt and Popov (1989) suggest that the link plastic rotation, γ_p , at the ultimate limit state should be limited to 0.08 radians for short links and 0.02 radians for long links. Such limits are also indicated in the Eurocode 8 (CEN 2004). Centrally located links in an EBF are classified as short when the link length is less than 1.6 times the ratio of the plastic flexural capacity to the shear capacity, and are classified as long when the link length is greater than 3.0 times the ratio of the plastic flexural capacity to the shear capacity. When classifying short and long links, note that according to the EC8 (CEN 2004), the plastic flexural capacity, M_p , and shear capacity, V_p , of a link section without axial load can be calculated using Eqns. 3.2 and 3.3 respectively.

$$M_{p,link} = f_y b t_f (d - t_f) \quad (3.2)$$

$$V_{p,link} = \left(\frac{f_y}{\sqrt{3}} \right) t_w (d - t_f) \quad (3.3)$$

where f_y is the steel yield strength, b is the flange width, d is the section depth, t_f is the flange thickness and t_w is the web thickness.

In order to relate the plastic rotation, $\gamma_{p,link,i}$ of a link at level i to an equivalent plastic storey drift component, $\theta_{i,p}$, the following relationship (from Engelhardt and Popov 1989) can be used for EBF structures with links of length e_i centrally located within bays of length L_b (see Figure 3.1):

$$\theta_{i,p} = \frac{e_i \cdot \gamma_{p,link,i}}{L_b} \quad (3.4)$$

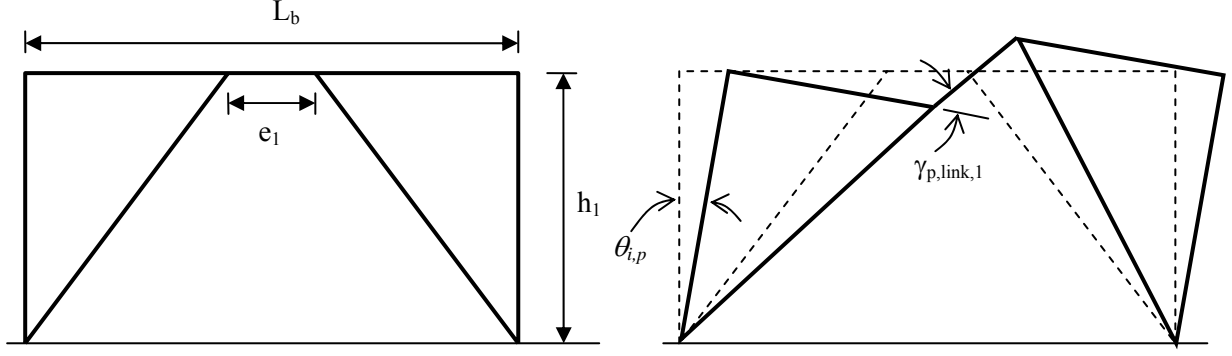


Figure 3.1. Geometrical layout (left) and plastic deformed shape (right) of an EBF structure with a central link.

The storey drift capacity at the ultimate limit state can be taken as the sum of the drift obtained from Eqn.3.4 with the storey yield drift. Expressions for the estimation of the storey yield drift of EBFs are presented in the next section. For structural deformation limits at the serviceability limit state, one could aim for elastic link response by setting the design storey drift to the yield drift, which can again be approximated using the expressions provided in the next subsection.

3.2. Equivalent Viscous Damping of EBF Structures

The equivalent viscous damping of a structure depends on its hysteretic properties. Assuming that a bi-linear hysteretic model with a 5% post-yield force-displacement stiffness ratio is reasonably representative of the non-linear cyclic behaviour of steel EBF systems, the equivalent viscous damping can be estimated as:

$$\xi_{eq} = 0.07 \left(1 + \frac{1.17(\mu - 1)}{1 + e^{\sqrt{\mu - 1}}} \right)^2 - 0.02 \quad (3.5)$$

Where μ is the displacement ductility demand. The above equation has been derived from the expression for displacement reduction factors developed by Maley et al. (2012) and should only be used together with the damping-dependent spectral reduction expression of Eqn. 2.1. Eqn.3.5 assumes 5% elastic damping and future research should consider what changes are required to account for the lower values of elastic damping typically predicted in steel structures.

From inspection of Eqn. 3.5 it is clear that the ductility demand for a certain limit state is required in order to estimate the damping. The ductility demand at a given storey can be taken as the storey drift demand, θ_i , divided by the storey yield drift, $\theta_{i,y}$, as shown in Eqn. 3.6:

$$\mu_i = \frac{\theta_i}{\theta_{i,y}} \quad (3.6)$$

The storey drift demand can be obtained by taking the differences in adjacent storey displacements obtained from Eqn. 3.1. The storey yield drift should instead be estimated with account for the following three deformation components: (i) the link deformation, (ii) the brace axial deformations, and (iii) column axial deformations below the storey under consideration. Through simplified considerations of these components, the following expression for the storey yield drift is proposed:

$$\theta_{i,y} = \frac{2\delta_{v,i}}{L_b - e_i} + \frac{2k_{br,i}\epsilon_y}{\sin 2\alpha_{br,i}} + \frac{2k_{cols,i-1}\epsilon_y(h_i - h_s)}{L_b} \quad (3.7)$$

where $k_{br,i}$ is the ratio of the design stress (due to DBD seismic forces) to the yield stress of the brace

section at level i , as per Eqn.3.8, $k_{cols,i-1}$ is the average ratio of the design stress to the yield stress in the column sections up to (but excluding) the level under consideration, as per Eqn.3.9, and $\delta_{v,i}$ is the vertical displacement of the end of the link at level i due to elastic deformations that can be estimated using Eqn.3.10 or Eqn. 3.11 for short or long links respectively.

$$k_{br,i} = \frac{N_{E,br,i}}{N_{Rs,br,i}} \quad (3.8)$$

$$k_{cols,i-1} = \frac{1}{i-1} \sum_{j=1}^{j=i-1} \frac{N_{E,col,j}}{N_{Rs,col,j}} \quad (3.9)$$

$$\delta_{v,i} = 0.577F_y A_{v,i} \left(\frac{e_i^2 (L_b - e_i)}{24EI_i} + \frac{e_i}{2GA_{v,i}} \right) \quad (3.10)$$

$$\delta_{v,i} = M_{p,i} \left(\frac{e_i (L_b - e_i)}{12EI_i} + \frac{1}{GA_{v,i}} \right) \quad (3.11)$$

In the above equations $N_{E,br,i}$ is the DBD axial force in the brace, $N_{Rs,br,i}$ is the brace section resistance at level i , $N_{E,col}$ is the DBD axial force in the column, $N_{Rs,col}$ is the column section resistance, I_i and $A_{v,i}$ are respectively the second moment of inertia and shear area of the link at level i , and $M_{p,i}$ is the plastic section moment resistance of the link at level i .

Upon inspection of Eqn.s 3.8 and 3.9, it is seen that to proceed with DBD, one should know the ratio of the design seismic force to the section resistance of braces and columns. A keen engineer will recognise that these ratios are a design choice, and provided that final sections are sized to respect initial estimates of the $k_{br,i}$ and $k_{cols,i-1}$ ratios, any value below 1.0 could be fine. In practice, however, it is difficult to provide a very efficient design solution without undertaking some iteration and to this extent, a starting value of 0.25 for both $k_{br,i}$ and $k_{cols,i-1}$ should lead to good results.

Eqn. 3.7 can therefore be used to approximate the storey yield drift of the EBF. This is useful for estimating both the storey drift capacity (in line with the recommendations of the previous section) and also the storey ductility demand using Eqn. 3.6. It is then proposed that the system ductility demand, μ_{sys} , be obtained factoring storey ductility demands, μ_i , by the design storey shear, V_i , and the design storey drift, θ_i , of all the n levels, in a work done approach shown in Eqn. 3.12:

$$\mu_{sys} = \frac{\mu_1 V_1 \theta_1 + \mu_2 V_2 \theta_2 + \dots + \mu_n V_n \theta_n}{\sum V_i \theta_i} \quad (3.12)$$

Even though the design storey shear is not initially known, note that the equation only actually requires the relative storey shear proportions. As such, the shears can be obtained from the equivalent lateral force profile of Eqn. 2.3 in which a unit base shear is specified.

Summarising, this section has presented equations for the estimation of the yield drift, ductility and equivalent viscous damping of EBF structures. Together with the design displacement profile of Eqn. 3.1, the Direct DBD approach described in Section 2 can now be applied. Note that when sizing links to satisfy the design forces, care should be taken to respect the EC8 recommendation that the ratio of the storey shear resistance to the design storey shear shall not vary by a factor greater than 1.25. Furthermore, it is recommended that to reduce the likelihood of concentrations in storey drift, the ratio should also not vary by more than a factor of 1.15 between adjacent storeys. The next section of this paper will report on a trial application of the methodology to a 10-storey case study building.

4. APPLICATION TO A 10-STOREY CASE-STUDY STRUCTURE

In order to gauge the ability of the Direct DBD methodology presented in the previous sections, a case study building is designed using the approach and then non-linear time-history (NLTH) analyses are undertaken to identify the likely non-linear dynamic response. Through comparison of displacements and drifts obtained from NLTH analyses with the design values, the potential ability of the trial methodology will be illustrated.

The case study building selected for this work is a regular 10-storey building shown in Figure 4.1. The building possesses a uniform storey height of 3.5m and bay lengths of 6m. Four identical EBFs are provided to resist lateral loads in each of the orthogonal directions. The storey weight is estimated as 4600kN (1150kN per frame) and this is assumed to be the same at every floor. Steel grade S450 is assumed, with an elastic modulus of 205000MPa and an expected yield strength of 528MPa (obtained by factoring the characteristic yield strength by 1.2).

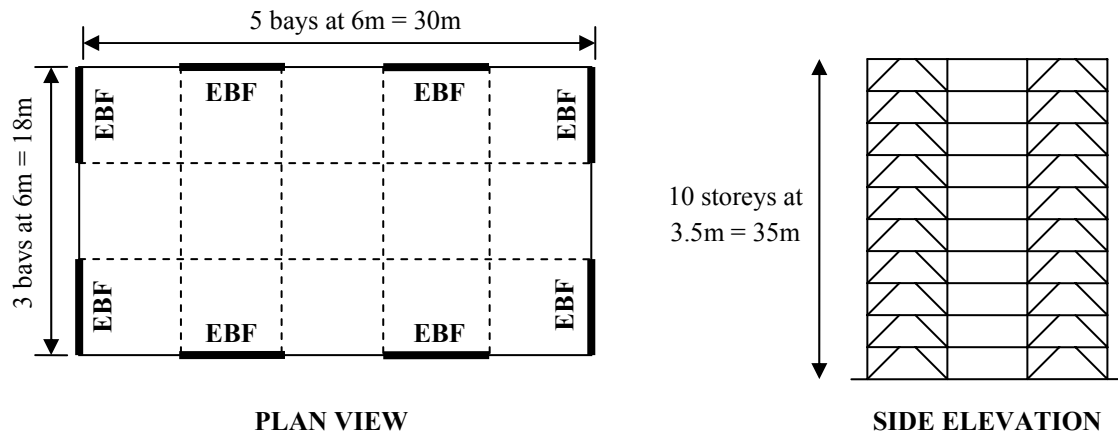


Figure 4.1. Plan view (left) and elevation (right) of the 10-storey case study EBF structure

The seismic hazard adopted for the ultimate (damage control) limit state design is the Eurocode 8 type 1 spectrum for soil type C, with a ground acceleration (a_g) of 0.3g. The acceleration and displacement response spectra are shown in Figure 4.2, together with the spectra of ten spectrum-compatible accelerograms selected for subsequent NLTH analyses. The record selection process is described in Maley et al. (2012a) and focussed on matching the design displacement spectrum.

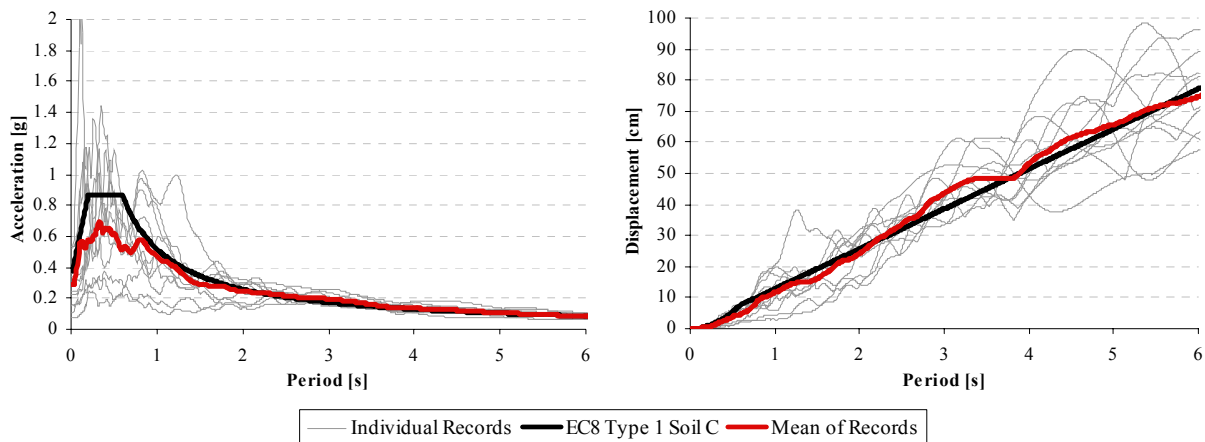


Figure 4.2. Design acceleration (left) and displacement (right) response spectra for the case study building, together with the average and individual spectra of 10 records selected for subsequent NLTH analyses.

For this case study building it is decided that short links are to be adopted, but the link length is not constant up the building height and is instead varied to optimise the design. Given that short links are to be used, the design plastic rotation of the links is taken to be 0.08rad and a non-structural drift limit of 2.5% is adopted for the ultimate limit state. An initial hypothesis is made about link section sizes and lengths as well as the coefficients $k_{br,i}$ and $k_{cols,i-1}$, so that the storey yield drifts can be estimated from Eqn. 3.7, the plastic storey drift capacity can be estimated from Eq.3.4 and the design displacement profile can be found from Eqn.3.1, with a higher mode drift reduction factor of 0.84.

The design displacement profile is then used to obtain storey drift and ductility demands at each level, as per Eqn.3.6. The system ductility is then found from Eqn.3.12 and the equivalent viscous damping from Eq.3.5. Through the procedure described in Section 2, the design base shear is then determined and a set of equivalent lateral design forces are obtained through Eqn.2.3, modified so that 10% of the base shear is lumped at roof level. Summing the lateral forces down the building provides the design shear force, V_i , at each level which leads to the required shear strength of links, $V_{link,i}$, as per Eqn. 4.1:

$$V_{link,i} = \frac{V_i h_s}{L_b} \quad (4.1)$$

where h_s is the storey height and L_b is the bay length (as per Figure 3.1). The section sizes initially assumed for the links are then checked. In addition, column and brace sizes are then selected, amplifying the DBD forces in line with capacity design principles. In this work the brace and column resistances were obtained using the Eurocode 3 (CEN 2005) guidelines. With the column and brace sizes set, and the link sizes updated, the initially assumed values of $k_{br,i}$, $k_{cols,i-1}$ and $\delta_{v,i}$ are then computed using Eqns. 3.8 to 3.10 and the design process is iterated until a stable solution is obtained. Table 4.1 presents the intermediate design results obtained for the final set of section sizes. The final section sizes selected for the links, braces and columns are reported in Table 4.2. Note that the design base shear for each frame is 964kN giving $V_b=3856$ kN for the whole building (8.4% the total weight).

Table 4.1. Intermediate design results for the 10-storey case study EBF structure

Level	Height, h_i (m)	Mass, m_i	Yield Drift	Drift capacity	Δ_i	θ_i	$m_i \Delta_i$	$m_i \Delta_i^2$	$m_i \Delta_i h_i$	Δ_d (m)	m_c (T)	H_c (m)
10	35.0	117.2	0.87%	1.54%	0.306	0.46%	35.9	11.0	1256.7	0.232	989	23.5
9	31.5	117.2	0.86%	1.66%	0.290	0.55%	34.0	9.9	1072.1			
8	28.0	117.2	0.79%	1.59%	0.271	0.64%	31.8	8.6	890.0			
7	24.5	117.2	0.77%	1.70%	0.249	0.74%	29.2	7.2	714.2			
6	21.0	117.2	0.78%	1.71%	0.223	0.83%	26.1	5.8	548.8			
5	17.5	117.2	0.67%	1.60%	0.194	0.92%	22.7	4.4	397.9			
4	14.0	117.2	0.65%	1.72%	0.162	1.02%	19.0	3.1	265.4			
3	10.5	117.2	0.58%	1.64%	0.126	1.11%	14.8	1.9	155.3			
2	7.0	117.2	0.57%	1.77%	0.087	1.20%	10.2	0.9	71.7			
1	3.5	117.2	0.49%	1.69%	0.045	1.29%	5.3	0.2	18.6			
Total:							229.0	53.0	5390.7			

Table 4.2. Final section sizes, ductility demands, shear demands and shear ratios for the case study structure.

Level	Brace Section	Column Section	Link Section	Link Length (m)	μ_i	$V_{d,i}$ (kN)	$V_{R,i}/V_{d,i}$
10	HE 180 A	HE 180 A	HE 120 A	0.50	1.49	222	1.36
9	HE 180 A	HE 180 A	HE 160 A	0.60	2.03	346	1.48
8	HE 180 A	HE 240 A	HE 180 A	0.60	3.00	461	1.33
7	HE 200 A	HE 240 A	HE 200 A	0.70	3.04	567	1.31
6	HE 200 A	HE 300 B	HE 180 B	0.70	3.03	661	1.38
5	HE 200 B	HE 300 B	HE 180 B	0.70	3.37	744	1.27
4	HE 200 B	HE 450 B	HE 200 B	0.80	3.51	812	1.36
3	HE 200 B	HE 450 B	HE 200 B	0.80	3.83	866	1.31
2	HE 200 B	HE 600 B	HE 200 B	0.90	3.34	903	1.23
1	HE 200 B	HE 600 B	HE 200 B	0.90	3.60	922	1.24

Table 4.2 also indicates the ductility demands (that lead to a system ductility of 3.4 and equivalent viscous damping of 21.6%) and the ratios of the storey shear resistance to the storey shear demand, which do not differ by more than a factor of 1.25 overall or by more than 1.15 in adjacent storeys.

5. PERFORMANCE OF THE DIRECT DBD SOLUTION

In order to gauge the performance of the design solution a series of NLTH analyses are undertaken. To do this, a 2D lumped-plasticity model is constructed in Ruaumoko (Carr 2009). Links are provided with bi-linear hysteretic properties, matching the design assumptions. Columns, braces and beam segments outside the link zone are modelled as elastic elements using the section properties obtained from manufacturers' tables. Masses are lumped at the column locations on every floor and floors are assumed to constrain the column nodes to translate together, with a rigid-diaphragm type behaviour. Link nodes are instead not constrained. Large displacement analyses are utilised and a gravity column is modelled in parallel to the EBF system so that P-delta effects are present. A Newmark integration scheme is adopted with an integration time step of 0.001s. A Rayleigh tangent-stiffness proportional damping model is used in line with the recommendations of Carr (2009) and Priestley et al. (2007), with 3% damping specified for the 2nd mode of vibration and a low value of 1.37% damping specified for the 1st mode of vibration to give the effect of 3% damping, using the recommendations of Priestley et al. (2007). The spectra of 10 records selected for the analyses were presented earlier in Section 4.

Figure 5.1 presents the peak storey displacements and drifts obtained from the NLTH analyses. Comparisons are made with the 1st mode design profiles as well as the design drift capacity. The 1st mode design drift profile is smaller than the design drift capacity as it is factored by the higher mode drift reduction factor, that was taken as 0.84, as reported earlier.

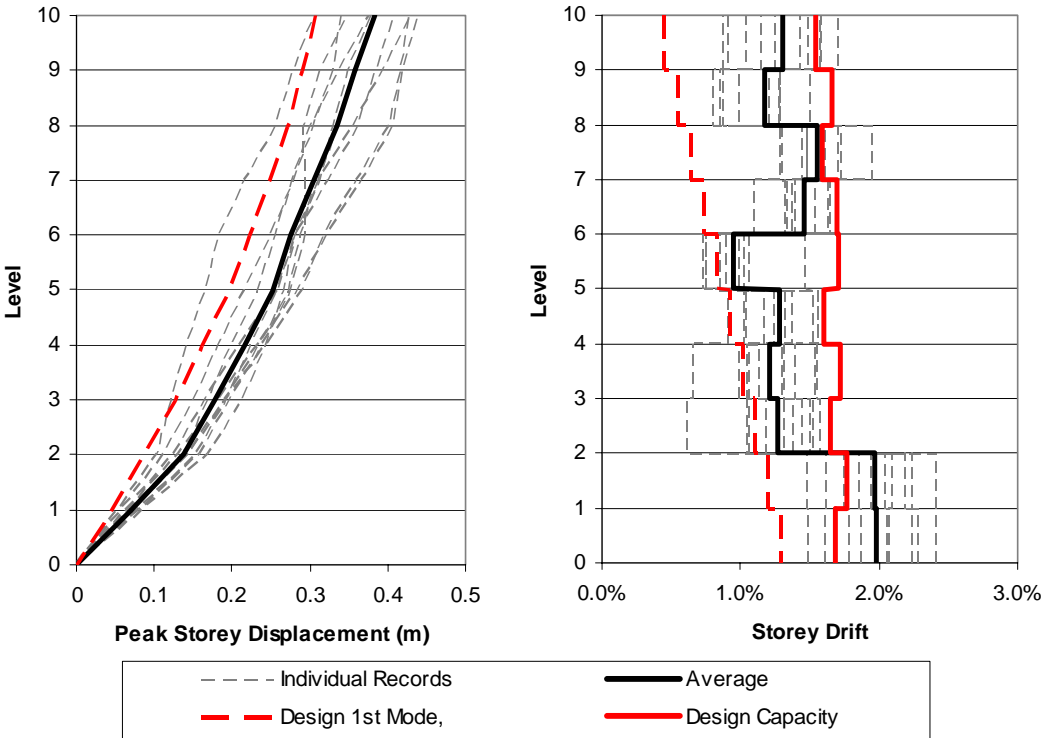


Figure 5.1. Peak storey displacements (left) and drifts (right) obtained from NLTH analyses of the 10-storey case study EBF structure, with comparisons to design values.

Reviewing the results in Figure 5.1 it can be concluded that the design methodology looks promising, since the average design drift profile is close to the design drift capacity. On the other hand, it can be noted that the 1st mode displacement and drift profiles are significantly less than the average

displacement and drift profiles. These differences might be attributed to higher mode effects, noting that the higher mode periods in EBF structures are relatively long, implying that their displacement and drift contributions could be significant. However, it could also be that improved expressions for the yield drift are necessary to better control the first mode response. As such, further research should be undertaken to investigate the behaviour more thoroughly and refine the trial DBD methodology.

6. CONCLUSIONS

In this paper, a trial Direct DBD procedure for steel EBF structures has been formulated. New expressions are proposed for the yield drift and the design displacement profiles of EBFs with K-braced configuration. Reference has been made to the literature for identification of suitable deformation limits and equivalent viscous damping expressions. The trial procedure has been applied to a 10-storey EBF structure and non-linear time-history analyses have been undertaken to gauge the performance of the methodology. Results of the analyses indicate that the trial methodology performs reasonably well but future research is required to develop and test the trial procedure more thoroughly.

REFERENCES

- Carr, A. (2009). Ruaumoko Theory Manual, University of Canterbury, New Zealand.
- CEN (2004). Eurocode 8 – Design Provisions for Earthquake Resistant Structures, EN-1998-1:2004, European Committee for Standardization, Brussels, Belgium.
- CEN (2005). Eurocode 3: Design of steel structures - Part 1-1: General rules and rules for buildings, EN 1993-1-1:2005, European Committee for Standardization, Brussels, Belgium.
- Della Corte, G. and Mazzolani, F.M. (2008). Theoretical developments and numerical verification of a displacement-based design procedure for steel braced structures. *14th World Conference on Earthquake Engineering*, Beijing, China.
- Engelhardt, M.D., Popov, E.P., (1989). Behavior of Long Links in Eccentrically Braced Frames. Report EERC-89-01, Earthquake Engineering Research Centre, Berkeley, California, U.S.A.
- Goggins, J.G. and Sullivan, T.J. (2009). Displacement-based seismic design of SDOF concentrically braced frames, in STESSA 2009, Mazzolani, Ricles & Sause (eds), Taylor & Francis Group, pp. 685-692.
- Maley, T.J., Roldán, R., Lago, A., Sullivan, T.J. (2012a). Effects of response spectrum shape on the response of steel frame and frame-wall structures. (*in press*), IUSS Press, Pavia, Italy.
- Maley, T.J., Sullivan, T.J., Pampanin, S. (2012). Seismic Design of Mixed MRF Systems, (*in press*), IUSS Press, Pavia, Italy.
- Pennucci, D., Sullivan, T.J., Calvi, G.M., (2011). Displacement Reduction Factors for the Design of Medium and Long Period Structures. *Journal of Earthquake Engineering*, **15:S1**, 1-29.
- Priestley, M.J.N. (1993). Myths and Fallacies in Earthquake Engineering – Conflicts Between Design and Reality *Bulletin of the NZ National Society for Earthquake Engineering*, New Zealand, **26:3**, 329-341.
- Priestley, M.J.N., Calvi, G.M., and Kowalsky, M.J. (2007). Displacement Based Seismic Design of Structures, IUSS Press, Pavia, Italy.
- Roeder, C.W., Popov, E.P., (1977). Inelastic Behavior of Eccentrically Braced Steel Frames Under Cyclic Loadings. Report EERC-77-18, Earthquake Engineering Research Centre, Berkeley, California, U.S.A.
- Salawdeh, S. (2012). Seismic design of concentrically braced steel frames. PhD thesis, National University of Ireland, Galway, Ireland, 280pages.
- Shibata, A. and Sozen, M. (1976). Substitute structure method for seismic design in reinforced concrete. *ASCE Journal of Structural Engineering* **102:1**, 1–18.
- Sullivan, T.J., Calvi, G.M., Priestley, M.J.N. and Kowalsky, M.J. (2003). The limitations and performances of different displacement based design methods, *Journal of Earthquake Engineering*, **7:S11**, pp201-241.
- Sullivan, T.J., Maley T., Calvi G.M. (2011). Seismic response of steel moment resisting frames designed using a Direct DBD procedure. *8th International Conference on Structural Dynamics, Eurodyn2011*, paper No.730.
- Sullivan, T.J. Priestley, M.J.N., Calvi, G.M., *Editors* (2012). A Model Code for the Displacement-Based Seismic Design of Structures, DBD12, IUSS Press, Pavia, Italy.
- Whittaker, A., Uang, C.M., Bertero, V.V. (1987)., Earthquake Simulation Tests and Associated Studies of a 0.3-Scale Model of a Six-Story Eccentrically Braced Steel Structure. Report EERC-87-02, Earthquake Engineering Research Centre, Berkeley, California, U.S.A.
- Wijesundara, K. (2009). Design of concentrically braced steel frame with RHS shape braces. PhD thesis, ROSE School, IUSS Pavia, Italy, 345pages.